

## DESIGN OF THE CONTINUOUS CONTACT LOOSE RIDING RINGS ON SUPPORT BLOCKS INCLUDED IN THE SUPPORTING SYSTEMS OF ROTARY DRUMS

Cornel MARIN<sup>1</sup>, Gheorghe ENE<sup>2</sup>

<sup>1</sup> VALAHIA University of Târgoviste, E-mail: marin\_cor@yahoo.com

<sup>2</sup> POLITEHNICA University of Bucharest, E-mail: ghene01@yahoo.com

**Abstract** The rotary drums are technological equipments used in manufacturing clinker cement materials using the LEPOL process, cooling cement clinker, cooling burnt pyrites exhausted from roasting furnace lines of sulfuric acid, cooling alumina discharged from calcination ovens, cooling lime exhausted from lime ovens, cooling slag from chemical fertilizer furnaces, etc. Rotary drums are also used in mixing of powder or granular materials, separation and enrichment of ore, coal, etc., washing ores and other minerals, crystallization and extraction of sugar from sugar beets, etc., drying various raw materials for cement clinker, clay, marl, furnace slag, coal, grain, etc.. This paper presents some contributions to the design and verification of continuous contact loose riding rings mounted on support blocks included in the equipment's bearing group.

**Keywords:** supports groups, aggregates with rotary drum, polar diagrams

### 1. OVERVIEW

The rotary drums support system is represented by continuous contact loose riding rings mounted on support blocks. They are important elements because in this way the loads are transmitted continuously from drum to the riding rings. This solution is used in case of very large (diameter 4 ... 5 m) and heavy aggregates (mass 35 ... 50 t) with large thermal expansion. These drums involve particular challenges in fabrication, installation and maintenance, considering that their average lifetime should be between 15 and 20 years with no major service [11]. Each bearing group consists of two cylindrical bearings placed symmetrically with respect to the vertical plane containing the axis of the drum (Fig. 1).

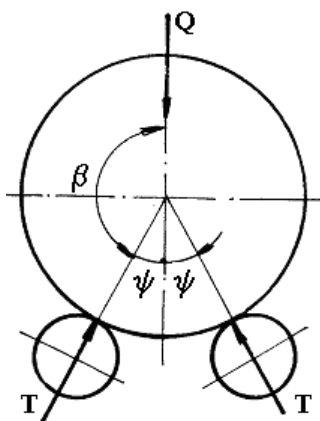


**Fig. 1 The riding rings supporting scheme**

The optimal position angle of the bearings with respect to the vertical diametral plane of the drums is  $\psi = 30^\circ$ . For higher values the roller's load increases and for lower ones the drum's stability decreases too much.

In the riding rings appear stresses due to bending moments, axial forces on the ring section and contact forces in areas between ring and roller bearings.

The size of these stresses depends on the method of mounting the ring on the drum.

Below are given the necessary design elements for all mentioned mounting methods. Analyzing a series of papers [1, 4, 5, 10, 11, 12, 13, 14] one tried to summarize the calculations in order to facilitate their practical use.

### 2. DETERMINING BENDING MOMENTS AND PLOTTING OF POLAR DIAGRAMS

In this case the loads transmitted from the drum to the riding ring are radial and symmetric with respect to the vertical diametral plane. They are distributed on the arc corresponding to the center angle  $2\pi - 2\alpha$  (Fig. 2) and have a continuously cosine variation:

$$q = q_0(\cos \alpha - \cos \varphi) \quad (1)$$

where  $q$  is the distributed load per unit length of circumference, N / m;

$\varphi$  – angle corresponding to the current ring's section

$\alpha$  - angle from which the load  $q_0$  on the ring starts

$q_0$  – the determined load [1,2,3] given by:

$$q_0 = \frac{Q}{R\left(\pi - \alpha - \frac{3}{2} \sin 2\alpha\right)} \quad (2)$$

$Q$  – load in support, N

$R$  – average radius of the riding ring circumference, m

The angle  $\varphi$  varies in the range  $\alpha \leq \varphi \leq \pi$ .

For  $\varphi = \pi$ , the load  $q$  has the form [1], given by:

$$q_\pi = q_0(1 + \cos \alpha) = \frac{Q}{R} \cdot \frac{1 + \cos \alpha}{\pi - \alpha - \frac{3}{2} \cdot \sin 2\alpha} \quad (3)$$

The bending moments caused by load  $q$  on the ring are determined using the following relations (fig. 2):

- for  $0 \leq \varphi \leq \alpha$ :  
 $M = M_0 + N_0 R (1 - \cos \varphi)$ ; (4)

- for  $\alpha \leq \varphi \leq \beta$  :  
 $M = M_0 + N_0 R (1 - \cos \varphi) + M_q$  (5)

- for  $\beta \leq \varphi \leq \pi$  :  
 $M = M_0 + N_0 R (1 - \cos \varphi) + M_q - TR \sin(\varphi - \beta)$  (6)

where  $M_0$ ,  $N_0$  and  $M_q$  are determined by the relationships [12]:

$$M_0 = \frac{q_0 R^2}{\pi} \left[ \frac{5}{4} \sin \alpha \cos \alpha + (\pi - \alpha) \left( \frac{3}{4} + \frac{1}{2} \cos^2 \alpha - \cos \alpha - \sin \alpha \right) \right] + \frac{TR}{\pi} [1 + \cos \beta - (\pi - \beta) \sin \beta]$$
 (7)

$$N_0 = \frac{q_0 R}{4\pi} \left[ 3 \sin \alpha \cos \alpha + (\pi - \alpha) (1 + 2 \cos^2 \alpha) \right] + \frac{T}{\pi} (\pi - \beta) \sin \beta$$
 (8)

$$M_q = q_0 R^2 \left[ \cos \alpha - \frac{1}{2} \cos \varphi - \frac{\varphi - \alpha}{2} \sin \varphi - \frac{1}{2} \cos \alpha \cos(\varphi - \alpha) \right]$$
 (9)

The force  $T$  is determined from equilibrium equation on vertical direction (fig.1):

$$T = \frac{Q}{2 \cos \psi} = - \frac{Q}{2 \cos \beta}$$
 (10)

One takes into account that in these situations the load acts only on the lower half of the ring (fig. 3). Thus in the above relations (7), (8), (9), one will use the particular value  $\alpha = 90^\circ$ .

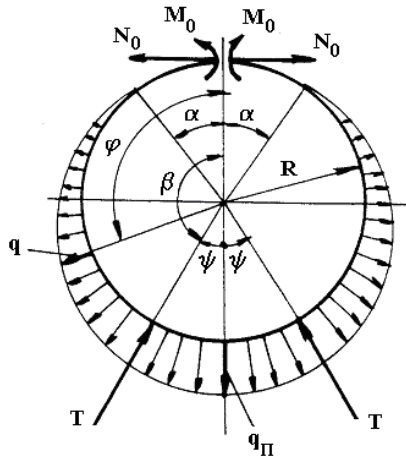


Fig. 2 The loading scheme for loose riding rings with continuous contact

In this case relation (1) becomes:

$$q = -q_0 \cos \varphi = -\frac{2Q}{\pi R} \cos \varphi$$
 (11)

where:  $q_0 = \frac{2Q}{\pi R}$  (12)

Relations (7), (8), (9) become:

$$M_0 = -\frac{QR}{\pi} \left[ \frac{2}{\pi} - \frac{1}{4} + \frac{1}{2 \cos \beta} - \frac{\pi - \beta}{2} \operatorname{tg} \beta \right]$$
 (13)

$$N_0 = -\frac{Q}{2\pi} \left[ \frac{1}{2} + (\pi - \beta) \operatorname{tg} \beta \right]$$
 (14)

$$M_q = -\frac{QR}{\pi} \left[ \cos \varphi + \frac{2\varphi - \pi}{2} \sin \varphi \right]$$
 (15)

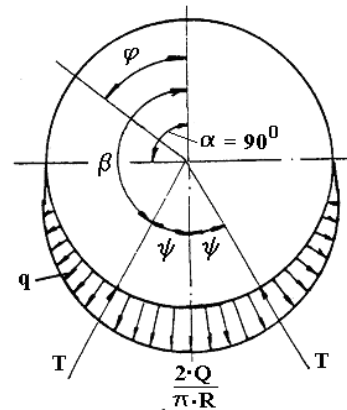


Fig. 3 The lower half loading scheme for loose riding rings with continuous contact

For the particular value  $\psi = 30^\circ$  ( $\beta = 150^\circ$ ) relations (13), (14) become:

$$M_0 = 0,0128 \cdot Q \cdot R$$
 (16)

$$N_0 = -0,013 \cdot Q$$
 (17)

By introducing these expressions into relation (4), (5), one obtains:

- for  $0 \leq \varphi \leq \alpha$ :  
 $M = QR [0,01287 - 0,013(1 - \cos \varphi)]$ ; (18)

- for  $\alpha \leq \varphi \leq \beta$  :  
 $M = QR [0,01287 - 0,013(1 - \cos \varphi)] + M_q$  (19)

- for  $\beta \leq \varphi \leq \pi$  :  
 $M = QR [0,01287 - 0,013(1 - \cos \varphi)] + M_q - TR \sin(\varphi - \beta)$  (20)

The extreme values of the bending moments are:

$$M_{min} = -0,0256 \cdot Q \cdot R \quad (\text{for } \varphi = 104^\circ)$$
 (21)

$$M_{max} = +0,0633 \cdot Q \cdot R \quad (\text{for } \varphi = \beta = 150^\circ)$$
 (22)

The polar bending moments diagram is plotted in fig.4.

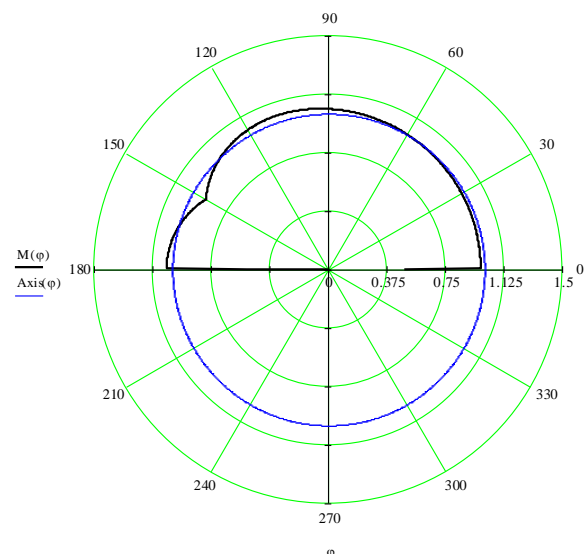


Fig. 4. The bending moment polar diagram for continuous contact riding rings

In the last case (when ring is loaded only on the lower half, fig. 3), the bending moments are:

$$M = K \cdot Q \cdot R \quad N.m \quad (23)$$

where K is determined using relations [11], [12]:

- for  $0 \leq \varphi \leq \alpha$ :

$$K = -\frac{1}{\pi} \left[ \frac{2}{\pi} + \frac{1}{2 \cos \beta} - \left( \frac{1}{4} + \frac{\pi - \beta}{2} \operatorname{tg} \beta \right) \cos \varphi \right] \quad (24)$$

- for  $\alpha \leq \varphi \leq \beta$ :

$$K = -\frac{1}{\pi} \left[ \frac{2}{\pi} + \frac{1}{2 \cos \beta} + \left( \frac{3}{4} - \frac{\pi - \beta}{2} \operatorname{tg} \beta \right) \cos \varphi + \frac{2\varphi - \pi}{2} \sin \varphi \right] \quad (25)$$

- for  $\beta \leq \varphi \leq \pi$ :

$$K = -\frac{1}{\pi} \left[ \frac{2}{\pi} + \frac{1 - \pi \sin(\varphi - \beta)}{2 \cos \beta} + \left( \frac{3}{4} - \frac{\pi - \beta}{2} \operatorname{tg} \beta \right) \cos \varphi + \frac{2\varphi - \pi}{2} \sin \varphi \right] \quad (26)$$

Using these relations, for the particular usual case  $\psi = 30^\circ$  ( $\beta = 150^\circ$ ) one obtains the maximum and minimum values:

- for  $\varphi = 150^\circ$ ,  $K_{max} = 0,086$  corresponding to the maximum moment one obtains:

$$M_{max} = +0,0633 \cdot Q \cdot R$$

- for  $\varphi = 104^\circ$ ,  $K_{min} = -0,068$  corresponding to the minimum moment one obtains:

$$M_{min} = -0,0256 \cdot Q \cdot R$$

The polar bending moments diagram is identical to the one plotted in figure 4.

Using these relations, for the particular case  $\psi = 45^\circ$  ( $\beta = 135^\circ$ ) one obtains the maximum and minimum values :

- for  $\varphi = 135^\circ$ ,  $K_{max} = 0,0352$  corresponding to the maximum moment

- for  $\varphi = 180^\circ$ ,  $K_{min} = -0,1788$  corresponding to the minimum moment

The polar bending moments diagram is plotted in fig. 5.

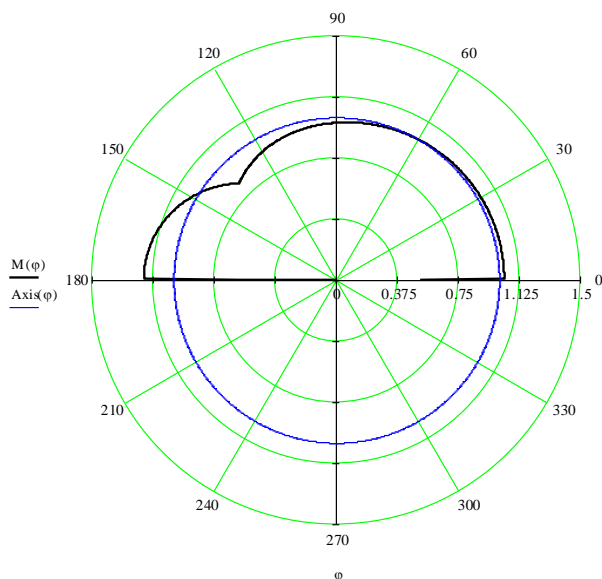


Fig. 5. The bending moment polar diagram for continuous contact riding rings ( $\psi = 45^\circ$ ).

Paper [10] recommends for loose riding rings, with continuous contact ( $\psi = 30^\circ$ ) the following values of K:  $K_{max} = 0,08$  și  $K_{min} = -0,03$  (27)

Thus, the K coefficient (used in relation [23])  $K = M/Q \cdot R$  is determined using the following methods:

**a) P.W.NIES Method [15]**

- for  $0 \leq \theta \leq \psi$ :

$$K = \frac{1}{2\pi} \left[ (\pi - \psi) \operatorname{tg} \psi \cos \theta - \frac{\cos \theta}{2} - \theta \sin \theta - \frac{1}{\cos \psi} \right]; \quad (28)$$

- for  $\psi \leq \theta \leq \pi$

$$K = \frac{1}{2\pi} \left[ (\pi - \psi) \operatorname{tg} \psi \cos \theta - \frac{\cos \theta}{2} - \theta \sin \theta - \frac{1}{\cos \psi} \right] + \frac{\sin(\theta - \psi)}{2 \cos \psi} \quad (29)$$

where  $\theta$  is current angle of section.

The behaviour of K -coefficient is presented in figure 6. One can observe from this figure that :

- for  $\theta = \psi = 30^\circ$ ,  $K_{max} = 0,086$  is obtained corresponding to the maximum moment:

$$M_{max} = +0,0633 \cdot Q \cdot R$$

- pentru for  $\theta \approx 83^\circ$ ,  $K_{min} = -0,068$  is obtained, corresponding to the minimum moment:

$$M_{min} = -0,0256 \cdot Q \cdot R$$

**b) S.B.KANTOROVICI Method [12]**

- for  $0 \leq \varphi \leq \beta$

$$K = -\frac{1}{2\pi} \left\{ \frac{1}{\cos \beta} + \varphi \sin \varphi + \left[ \frac{1}{2} - (\pi - \beta) \operatorname{tg} \beta \right] \cos \varphi \right\}; \quad (30)$$

- for  $\beta \leq \varphi \leq \pi$

$$K = -\frac{1}{2\pi} \left\{ \frac{1 - \pi \sin(\varphi - \beta)}{\cos \beta} + \varphi \sin \varphi + \left[ \frac{1}{2} - (\pi - \beta) \operatorname{tg} \beta \right] \cos \varphi \right\} \quad (31)$$

where  $\varphi$  is current angle of section.

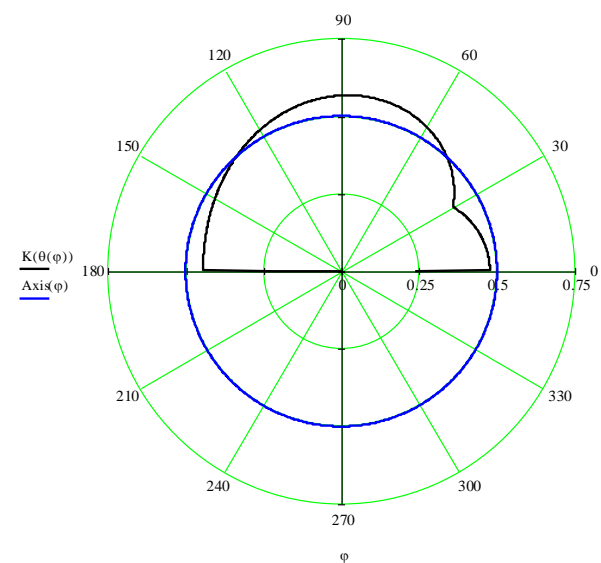
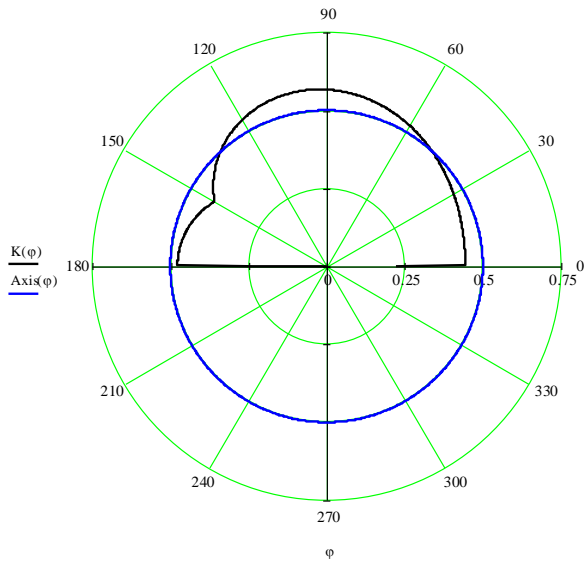


Fig. 6. The polar diagram of  $K(\theta)$  for continuous contact riding rings ( $\psi = 30^\circ$ ).



**Fig. 7. The polar diagram of  $K(\theta)$  for continuous contact riding rings ( $\psi = 30^\circ$ )**

With these expression one obtains:

- for  $\varphi = \beta = 150^\circ$   $K_{max} = 0,0857$  ;
- for  $\varphi = \beta = 96^\circ 45'$   $K_{min} = -0,0683$ .

The behaviour of  $K$  -coefficient is presented in figure 7. We observe that this figure has the same shape with figure 6, but rotated with  $180^\circ$  because:  $\beta = \varphi = \pi - \theta$  and  $\pi - \psi$ .

## 5. CONCLUSIONS

- The analysis of riding rings bending moments diagrams in Figures 4...6 shows that the most loaded section of the ring is the one corresponding to the contact with the supporting rollers, like in the case of loose rings mounted on support blocks.
- The originality of paper consists in plotting the bending moment polar diagrams using the relations found in the specialized literature and the features of MATHCAD software.
- One can observe in the diagrams presented by figures 5 and 6 that for a  $15^\circ$  angle increase, the bending moments increase 4 times. This justifies the recommendations referring to a  $30^\circ$  limiting value of the position angle.

## BIBLIOGRAPHY

- [1] Renert, M., Calculul și construcția utilajului chimic, vol.II, Editura Didactică și Pedagogică, București, 1971.
- [2] Beilich, E., Becherescu, D., Cuptoare și utilaje în industria silicaților, vol. 1, Cuptoare, Editura Didactică și Pedagogică, București, 1973.
- [3] Teoreanu, I., Beilich, E., Becherescu, D., Rehner, H., Instalații termotehnologice (lianți, sticlă, ceramică), Editura Tehnică, București, 1979

- [4] Iordache, Gh., Ene, Gh., Rasidescu, M., Utilaje pentru industria materialelor de construcții, Editura Tehnică, București, 1987.
- [5] Jinescu, V. V., Utilaj tehnologic pentru industrii de proces IV, Editura Tehnică, București, 1989.
- [6] Duda V. H. Cement-Data-Book, Berlin, Londra, Bauverlag GMBH, 1976.
- [7] Levcenco, P. L., Rasciotî pecei i sușil silikatnoi promișlenosti, Izd.Vișșaiia șkola, Moskva, 1968.
- [8] Rogovoi, M. M., Kondakova, M. M., Saganovskii, N., Rasciot i zadaci po teplotehneskomu obordovaniiu predpriatii promișpenosti stroitelniș materialov, Izd.Stroizdat, Moskva, 1975.
- [9] Dăscălescu, A., Uscarea și aplicațiile ei industriale, Editura Tehnică, București, 1964.
- [10] Domașnev, A. D., Utilaje pentru industria chimică, (traducere din limba rusă), Ed.Tehnică, București, 1962.
- [11] Boganov, A. I., Vrașciaiusciesia peci țementnoi promișlenosti, Izd. Mașinostroenie, Moskva, 1965.
- [12] Kantorwitsch, S. B., Die Festigkeit der Apparate und Maschinen fur die Chemische Industrie, Veb Verlag Technik, Berlin, 1955.
- [13] Iordache, Gh., Ene, Gh., Agregate cu tambur rotativ. Îndrumar de proiectare, IPB, 1985.
- [14] Ene, Gh., Marin, C., Influence of uneven support groups to reaction values and bending diagrams of rotary kilns, The Scientific Bulletin of VALAHIA University. MATERIALS and MECHANICS, No. 1, (6), 2008, p. 151-157.
- [15] Nies, P. W., Die Berechnung der Drehofenlanfringe, Zement, 31,1942,p. 23.